Research Square

Preprints are preliminary reports that have not undergone peer review.
They should not be considered conclusive, used to inform clinical practice,
or referenced by the media as validated information.

Postnatal Growth of Angular Trajectory of Vestibular Aqueduct in a Chinese Cohort: Association with Other Radiological Indices

Ziying Xu
Huazhong University of Science and Technology
Xingqian Shen
Huazhong University of Science and Technology
Xuanyu Shi
Huazhong University of Science and Technology
Qin Liu
Huazhong University of Science and Technology
Xiaoye Chen
Huazhong University of Science and Technology
Kaijun Xia
Huazhong University of Science and Technology
Yingzhao Liu
Huazhong University of Science and Technology
Yangming Leng
Huazhong University of Science and Technology
Cen Chen
Huazhong University of Science and Technology
Ping Lei
Huazhong University of Science and Technology
Bo Liu
liuboent@hust.edu.cn

Huazhong University of Science and Technology

Research Article

Keywords: Angular trajectory of the vestibular aqueduct, Postnatal development, Vestibular aqueduct, Endolymphatic sac, High-resolution computer tomography, Chinese?

Posted Date: September 10th, 2026

DOI: https://doi.org/10.21203/rs.3.rs-10637580/v1

License: This work is licensed under a Creative Commons Attribution 4.0 International License.
Read Full License

Additional Declarations: No competing interests reported.

Postnatal Growth of Angular Trajectory of Vestibular Aqueduct in a Chinese Cohort: Association with Other Radiological Indices

Ziying Xu [1 †], Xingqian Shen [1 †], Xuanyu Shi [1], Qin Liu [1], Xiaoye Chen [1], Kaijun Xia [1], Yingzhao Liu [1], Yangming Leng [1,2], Cen Chen[3,4 *], Ping Lei [3,4 *], Bo Liu [1,2 *]

1: Department of Otorhinolaryngology-Head and Neck Surgery, Union Hospital, Tongji Medical College, Huazhong University of Science and Technology, Wuhan 430022, China

2: Hubei Province Clinical Research Center for Deafness and Vertigo, Wuhan 430022, China.

3: Department of Radiology, Union Hospital, Tongji Medical College, Huazhong University of Science and Technology, Wuhan 430022, China

4: Hubei Provincial Clinical Research Center for Precision Radiology & Interventional Medicine, Wuhan 430022, China

† Co-first authors/contributed equally to this work.

* Corresponding author:

Bo Liu, Email: liuboent@hust.edu.cn

Ping Lei, Email: leiping@hust.edu.cn;

Abstract

Background: The vestibular aqueduct plays a critical role in maintaining endolymphatic homeostasis, the anatomical alterations of which may be associated with endolymphatic hydrops and Meniere's disease (MD). The angular trajectory of the vestibular aqueduct (ATVA), reflecting the two distinct endolymphatic sac pathologies (hypoplastic and degenerative) observed in MD, serves as an imaging marker for MD subgrouping. However, its postnatal growth and relationship with other VA-related parameters in healthy individuals remain unclear. This study aimed to explore the postnatal growth and association of ATVA and other VA-related radiological parameters.

Methods: This retrospective study reviewed temporal bone high-resolution computer tomography (CT) scans of 190 subjects (380 ears) aged 0–18 years without otologic abnormality. ATVA, the vertical part of the posterior semicircular canal—the posterior fossa distance (PPD), and peri-VA pneumatization grading were measured. Generalized additive models for location, scale and shape (GAMLSS) were fitted to characterize ATVA dynamics,

with first-derivative analysis to determine the plateau age. Mixed-effects mediation models assessed the direct and indirect effects of age on ATVA and PPD.

Results: (1) Age was associated with a progressive decrease in ATVA, an increase in PPD, and a transition of peri-VA pneumatization from lower to higher levels. ATVA stabilized at 5.93 years. (2) ATVA was negatively correlated with PPD ($r = –0.144$, $p < 0.01$). PPD > 0.88 mm ruled out ATVA≥140° in 93.4% of ears. ATVA and PPD exhibited significant differences among varying pneumatization subgroups (all $p < 0.05$).

Conclusions: The VA exhibited a clear age-dependent developmental pattern. PPD > 0.88 mm effectively ruled out ATVA≥140° in this Chinese cohort. Peri-VA pneumatization underwent progressive postnatal development and showed significant associations with both ATVA and PPD, suggesting coordinated development among these three parameters.

Keywords: Angular trajectory of the vestibular aqueduct; Postnatal development; Vestibular aqueduct; Endolymphatic sac; High-resolution computer tomography; Chinese?

1. Introduction

Meniere's disease (MD) is a vestibular disorder characterized by episodic vertigo, fluctuating hearing loss, tinnitus, and aural fullness, with idiopathic endolymphatic hydrops (ELH) as its underlying histopathology [1]. Although its etiology and pathophysiological mechanisms have not yet been fully elucidated, dysfunction of the vestibular aqueduct (VA) and its contents, namely the endolymphatic duct (ED) and endolymphatic sac (ES), is considered one of the contributing factors to ELH [2-4]. The ES serves as a key homeostatic organ responsible for regulating endolymph volume and ionic composition within the inner ear [5-7], which affect the development and progression of MD. Recently, two histopathological subtypes of MD have been described in a human postmortem study: (i) MD with degenerative changes of the distal ES (MD-dg), and (ii) MD with hypoplastic ES (MD-hp) [5, 8].

The angular trajectory of the vestibular aqueduct (ATVA) can indirectly reflect the pathological types of the ES, thus serving as an imaging marker for the two afore-mentioned MD subtypes [9, 10]. The hypoplastic VA is first observable during the fetal period (gestational weeks 6–38) and is characterized by a short, nearly straight VA with no discernible angulation between the isthmus and the main body of the aqueduct [11]. Histopathologically, Kodama et al. demonstrated that the VA exhibits interindividual variation during the neonatal period and continues to elongate postnatally, extending posteriorly and inferiorly to assume its mature configuration [12]. This maturation process can be quantified radiologically by a progressive decline in the ATVA [10, 13].

Additionally, the vertical part of the posterior semicircular canal—the posterior fossa

distance (PPD)， which serves as a radiographic indicator of ES size, exhibits a significant negative correlation with the ATVA [3, 13-15]. Peri-VA pneumatization refers to the degree of air cell development in the petrous portion of the temporal bone adjacent to the VA[14]. Previous studies have demonstrated that MD patients exhibit significantly shorter PPD and a higher prevalence of poor peri-VA pneumatization compared with healthy individuals [14, 15]. In addition, Bächinger et al. further stratified the MD population and found that these alterations are more pronounced in the MD-hp subgroup than in the MD-dg subgroup [10].

Histopathological and radiographical evidence suggests marked inter-population differences in temporal bone size, orientation, and cranial base relationships, implying that the ATVA and VA-related parameters, as novel morphological indices, may follow population-specific growth trajectories [16-18].

The present study was designed to systematically characterize the postnatal development of peri-vestibular structures in a Chinese cohort using high-resolution computed tomography (CT), encompassing age-dependent dynamics in the ATVA, PPD, and peri-VA pneumatization, given the scarcity of such studies in the Chinese population. We aimed to explore the developmental trajectories and interrelationships of these parameters, thereby advancing the current understanding of peri-vestibular maturation and providing a radiological basis for the Understanding of VA-related disorders.

2. Participants and Methods

2.1. Participants

This retrospective study reviewed temporal bone high-resolution CT scans of patients aged 0 to 18 years who underwent imaging at Union Hospital, Tongji Medical College, Huazhong University of Science and Technology between 2015 and 2023 for non-otologic abnormality. A total of 190 subjects (380 ears) ultimately included.

The inclusion criteria were as follows: (1) age between 0 and 18 years; (2) available temporal bone CT scans with sufficient image quality to clearly identify the inner ear and vestibular aqueduct structures; (3) no obvious abnormalities on unenhanced CT. The exclusion criteria were: (1) audio-vestibular symptoms including hearing loss, vertigo, or tinnitus; (2) radiological signs of third-window syndrome; (3) known middle ear, inner ear, or cranial malformations; (4) temporal bone fracture; (5) history of otitis media;

2.2. Radiological Evaluation

2.2.1 High-resolution CT Protocols

CT examinations were performed using a 64-detector spiral CT scanner (Somatom Definition

AS+, Siemens, Forcheim, Germany). Subjects were scanned in the supine position with the scan plane parallel to the orbitomeatal line. The scan parameters were as follows: tube voltage 120 kV, CARE Dose 4D quality reference mAs: 180 mAs, slice thickness 0.6 mm, slice collimation 128 × 0.6 mm, pitch 0.5, field of view 150 mm, reconstruction increment 0.3 mm, and reconstruction kernel H60s. All images were transferred to a PACS workstation (Carestream Client, Carestream Health) for analysis.

2.2.2 Radiological Measurement

Software (available at https://github.com/DanielZuerrer/CoolAngleCalcJS) developed by Bächinger et al. for measurements of the angle of the vestibular aqueduct was used [8]. As described in Bächinger et al., all radiological measurements were performed on standardized axial reformatted images in the plane parallel to the lateral semicircular canal. A predefined shape (magenta shape, Figure 1A) was adjusted to fit the vestibule and the horizontal semicircular canal, thereby defining the first reference line (red line, Figure 1A). The second line (yellow line, Figure 1B) was manually adjusted to be parallel to the distal portion of the vestibular aqueduct near the operculum. The ATVA was determined as the angle between the first red line and the second yellow line (Figure 1A). According to the ATVA values, ears were further divided into three categories: ATVA ≤120°, 120°＜ATVA ＜140°, and ATVA ≥ 140° [10].

The PPD (Figure 1C) was assessed according to previously established methods [19]. Peri-vestibular aqueduct (peri-VA) pneumatization was categorized into three subtypes: type 1: large-cell pneumatization in the vicinity of the VA (Figure 1D); type 2: small-cell pneumatization in the vicinity of the VA (Figure 1E); and type 3: absence of air cells (Figure 1F) [14].

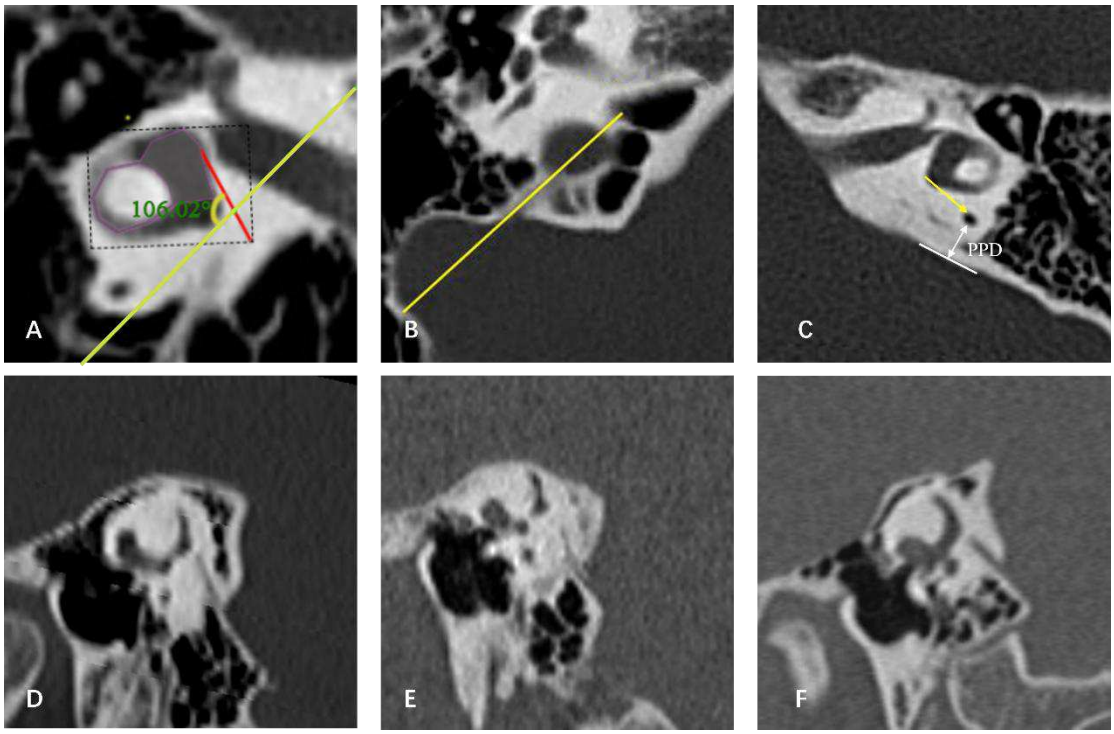


Fig.1 Measurement of the angular trajectory of the vestibular aqueduct (ATVA) and assessment of related radiological parameters. (**A**)The predefined shape is fitted to the vestibule and the horizontal semicircular canal. (**B**) The yellow line was manually adjusted to be parallel to the distal portion of the vestibular aqueduct. The ATVA refers to the angle between the red line and the yellow line. (**C**) Measurement of the vertical part of the posterior semicircular canal—posterior fossa distance (PPD). Yellow arrow: vertical part of the posterior semicircular canal; white curve: anterior boundary of the posterior fossa. (**D**) type 1: large-cell pneumatization in the vicinity of the VA; (**E**) type 2: small-cell pneumatization in the vicinity of the VA; (**F**) type 3: absence of air cells.

2.3 Statistical Analysis

All statistical analyses were performed using R software (version 4.5.3). Given that the ATVA and PPD data deviated from normality, they are summarized as median (interquartile range, IQR). Inter-rater reliability was quantified using ICC (continuous variables) and kappa (categorical variables). Group comparisons and interaural symmetry were evaluated using Kruskal-Wallis and Wilcoxon signed-rank tests, respectively, with Dunn's post-hoc correction for multiple comparisons. Receiver operating characteristic (ROC) curve analysis was performed to determine the optimal PPD cutoff for predicting ATVA $\geqslant 140^\circ$.

Age-specific reference curves for ATVA were constructed using generalized additive models for location, scale and shape (GAMLSS) [20], with the 90th percentile (P90) designated as the

threshold for identifying delayed development. The age at which ATVA maturation stabilized was determined via first-derivative analysis of the age spline, defined as the point where the rate of change ceased to differ from zero (i.e., d (ATVA)/d (age) = 0).

To explore the potential pathways through which age influences ATVA development, mixed-effects mediation models were fitted with subject-specific random intercepts to account for the correlation between bilateral ears. The average causal mediation effects (ACME), average direct effects (ADE), and the proportion mediated were estimated via quasi-Bayesian Monte Carlo simulations with 1,000 iterations. A p-value < 0.05 was considered statistically significant [21].

3. Results

3.1 Study Cohort and ATVA Distribution

This study included 190 subjects (380 ears), with 10 subjects per year of age. Inter-reader agreement was excellent for all parameters (ATVA ICC = 0.97; PPD ICC = 0.98; pneumatization kappa = 0.95). As shown in Table 1, the ATVA exhibited an age-dependent decrease during infancy and early childhood, declining from 129.8（120.6，153.5） at 0–1years of age to 98.1（87.0，105.1）by 4–5 years of age. After 5 years of age, the ATVA values tended to fluctuate without a consistent unidirectional trend. From 7 years of age onward, the proportion of ATVA ⩾ 140 ° remained at a low level, while 120 ° ＜ ATVA ＜ 140 ° consistently ranged between 15% and 30%.

Table 1. Cohort age distribution and corresponding ATVA and PPD values.

Age range(years)	PPD	ATVA	ATVA ≥140°	120 ° ＜ ATVA ＜ 140°	ATVA ≤120°
0-1	0.6（0.5，0.9）	129.8（120.6，153.5）	30%	50%	20%
1-2	0.7（0.4，1.2）	119.9（106.9，145.3）	25%	25%	50%
2-3	1.0（0.6，1.3）	121.2（106.7，136.9）	20%	35%	45%
3-4	1.1（0.8，2.0）	107.9（101.5，122.4）	10%	15%	75%
4-5	1.7（1.1，2.4）	98.1（87.0，105.1）	0%	5%	95%
5-6	2.0（1.0，2.6）	112.2（99.1，132.0）	10%	35%	55%
6-7	1.8（0.8，2.6）	114.1（101.8，137.3）	25%	10%	65%

7-8	2.0（1.1，2.5）	109.1（100.0，116.0）	5%	15%	80%
8-9	1.8（1.5，2.3）	103.3（97.5，115.2）	10%	10%	80%
9-10	1.7（1.2，2.8）	103.8（97.8，112.6）	0%	5%	95%
10-11	2.0（1.2，2.6）	105.9（98.8，122.7）	10%	20%	70%
11-12	2.7（1.9，3.8）	108.6（101.7，118.7）	0%	15%	85%
12-13	1.9（1.4，3.6）	106.7（94.2，121.6）	10%	10%	80%
13-14	2.1（1.2，3.1）	106.3（95.3，119.6）	5%	15%	80%
14-15	3.2（2.0，4.6）	114.0（93.9，126.9）	0%	30%	70%
15-16	1.9（1.1，3.6）	109.9（101.1，115.0	0%	10%	90%
16-17	2.1（1.1，5.1）	109.8（101.9，117.1）	5%	15%	80%
17-18	3.6（3.0，4.8）	111.1（96.9，117.2）	0%	15%	85%
18-19	2.8（1.4，3.7）	105.7 (98.5,123.0）	0%	25%	75%

Note：ATVA: The angular trajectory of the vestibular aqueduct; PPD: The vertical part of the posterior semicircular canal—the posterior fossa distance.

3.2 Interaural Symmetry

At the group level, no significant differences were observed between the left and right ears in ATVA ($p = 0.16$), PPD ($p = 0.18$), or peri-VA pneumatization grade ($p = 0.26$), indicating no systematic bias. At the individual level, however, substantial interaural discrepancies were noted, with a standard deviation of 16.9°. Discordant ATVA categorization between the two ears was observed in 29.5% of individuals. Furthermore, a negative correlation was found between age and the absolute interaural difference in ATVA ($r = –0.181$, $p = 0.012$), suggesting a gradual reduction in bilateral ATVA disparity with increasing age.

3.3 GAMLSS Derived Age-Specific ATVA Reference Table

To quantitatively characterize the age-dependent changes of ATVA during postnatal development, we fitted GAMLSS to establish age-specific reference percentiles. The final GAMLSS model revealed that the ATVA fell below 140° in 50% of individuals at 2 months of

age and in 90% at 4.45 years; below 130° in 50% at 0.75 years and in 90% at 16.8 years; and below 120° in 50% at 1.9 years, while a proportion of individuals (16.1%) did not reach an ATVA≤120° by 19 years of age（Table 1S）. In addition, we established age-specific screening thresholds for delayed ATVA development, with values exceeding the red warning line at the corresponding age raising concern for permanent ATVA hypoplasia (Figure 2A). First-derivative analysis of the ATVA age spline identified stabilization at 2,166 days (5.93 years), indicating the age at which VA development plateaus (Figure 2B).

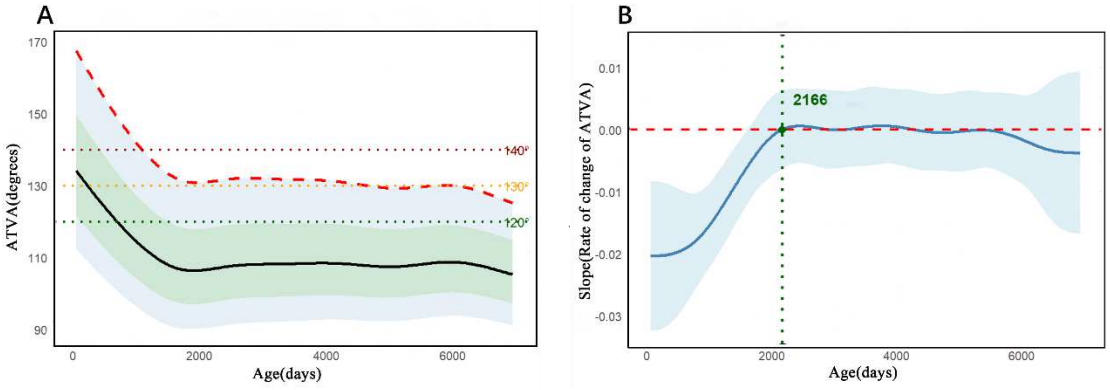


Fig.2 Age-specific ATVA reference curves and developmental trajectory. (**A**) GAMLSS-derived percentile reference curves for ATVA in healthy subjects aged 0–18 years. Green-shaded: P25–P75; blue-shaded: P10–P90; black solid line: median (P50); red dashed line: age-specific P90 screening threshold for delayed development. Horizontal dashed lines indicate cutoffs for ATVA＝120°, ATVA＝130°, and ATVA＝140°. (**B**) First-derivative plot with 95% confidence band (blue) from the final fitted GAMLSS. ATVA change plateaus (slope → 0) at approximately 2,166 days (5.93 years).

3.4 Association between ATVA and PPD

The ATVA showed a negative correlation with PPD ($r = –0.144$, $p < 0.01$). The optimal cutoff value (maximizing Youden index) of PPD for distinguishing ATVA≥140 from ATVA≤120 was 0.88 mm, yielding a sensitivity of 48.5%, a specificity of 88.0%, a positive predictive value of 32.7%, a negative predictive value (NPV) of 93.4%, and an area under the curve (AUC) of 0.702 (95% CI: 0.595–0.810) (Figure 3).

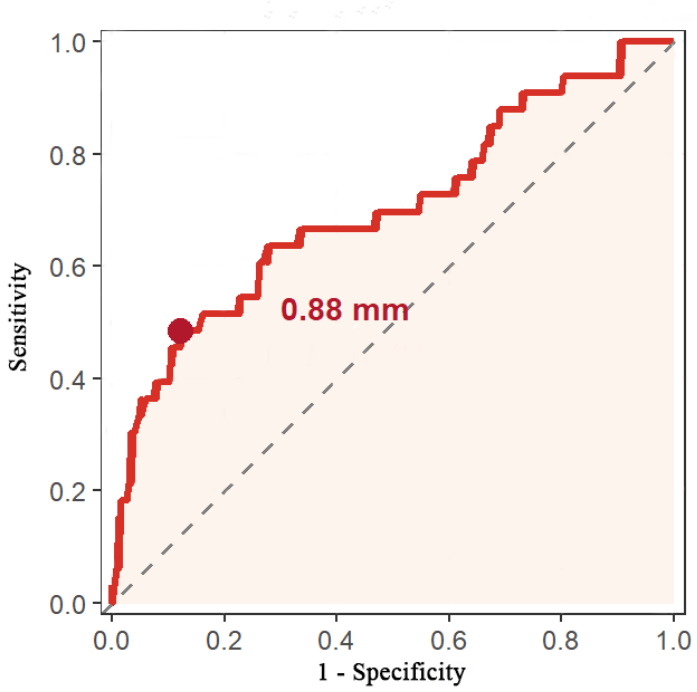


Fig.3 ROC curve of PPD for differentiating ATVA≥140 from ATVA≤120. The optimal cutoff was 0.88 mm, with a sensitivity of 0.48 and specificity of 0.88 (AUC = 0.702). The corresponding point is indicated on the curve.

3.5 Relationships among Age, ATVA, PPD, and Pneumatization Grade

Age showed a significant negative correlation with ATVA ($p < 0.001$), corresponding to a decrease of 0.77° per year, and a significant positive correlation with PPD ($p < 0.001$), corresponding to an increase of 0.12 mm per year. The distribution of pneumatization types shifted significantly with age: type 1 increased, while type 2 and type 3 decreased (Fig. 1S). The age of type 1 ears was significantly older than that of the other two types ($p < 0.01$), with no difference between type 2 and type 3 ($p = 1.00$) (Figure 4A). ATVA differed significantly across pneumatization subgroups: the mean ATVA in Type 2 was significantly lower than that in Type 3 ($p < 0.01$) and Type 1 ($p < 0.05$), whereas no significant difference was observed between Type 3 and Type 1 ($p = 0.615$) (Figure 4B). PPD also differed significantly across pneumatization subgroups: PPD in Type 3 was significantly lower than that in Type 2 ($p < 0.001$), and PPD in Type 2 was significantly lower than that in Type 1 ($p < 0.001$) (Figure 4C).

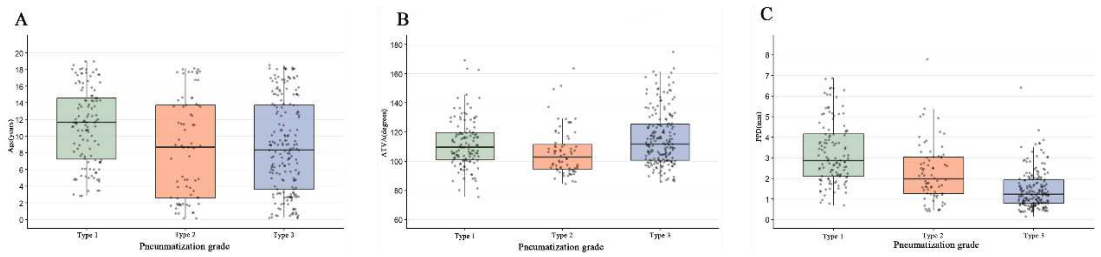


Fig.4 Distribution of age, ATVA, and PPD by mastoid pneumatization subgroups. (**A**) Age, (**B**) ATVA, and (**C**) PPD stratified by pneumatization type (Type 1: large-cell; Type 2: small-cell; Type 3: absent of cells). Statistically significant intergroup differences were found for all parameters.

Age exerted a significant direct effect on PPD ($p < 0.001$). Moreover, pneumatization grade significantly mediated the association between age and PPD ($p < 0.01$), with the mediation effect accounting for 7.6% of the total effect, indicating that a small proportion of the age-dependent increase in PPD was mediated through changes in pneumatization grade (Figure 5).

Age exerted a significant direct effect on ATVA ($p < 0.001$). However, neither pneumatization grade ($p = 0.35$) nor PPD ($p = 0.59$) mediated the relationship between age and ATVA (Figure 5).

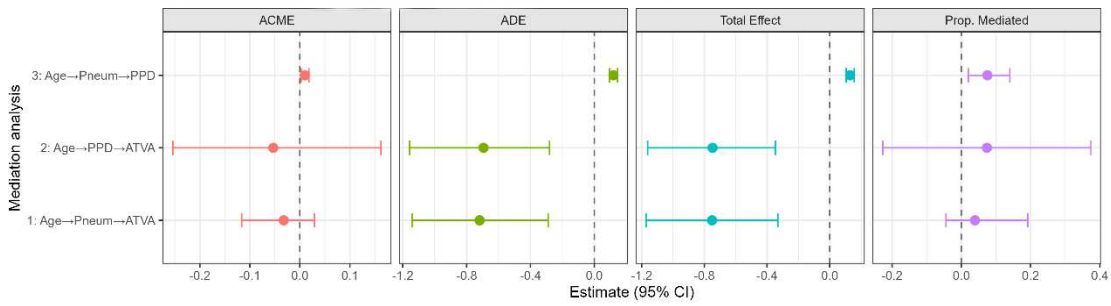


Fig.5 Mediation analysis of age, pneumatization grade, The vertical part of the posterior semicircular canal—the posterior fossa distance（PPD）, and The angular trajectory of the vestibular aqueduct（ATVA）. The mediation model shows that pneumatization grade significantly mediated the age–PPD association ($p < 0.01$), accounting for 7.6% of the total effect. However, neither pneumatization grade ($p = 0.35$) nor PPD ($p = 0.59$) mediated the age–ATVA relationship. ACE, average causal effect; ACME, average causal mediation effect; ADE, average direct effect.

4. Discussion

4.1 Postnatal developmental characteristics of ATVA and PPD–

In this retrospective analysis of 190 healthy subjects (0–18 years), we found that ATVA and PPD exhibited rapid postnatal maturation, with ATVA stabilizing at 5.93 years, a finding in line with prior reports [13, 22]. The age-dependent decline in ATVA mirrors the postnatal maturation of the VA and its contents (ED and ES). The ATVA≥140° is characterized by a short, straight configuration lacking angulation between the isthmus and the aqueduct proper [23]. With progressive maturation of the ED and ES, the VA elongates and courses obliquely in a posteroinferior direction, acquiring a distinct bend at the isthmus that defines the mature VA [8]. Our findings suggest that, in our cohort, the VA, ED, and ES reach maturation at approximately 6 years of age.

The ATVA maturation process in this study exhibited the following characteristics. (1) ATVA ≥140° was occasionally observed beyond 12 years of age, and 120°＜ATVA＜140° was consistently present across all age groups, with proportions ranging from 5% to 30%. By contrast, in the Juliano et al. cohort, no ATVA ≥140° was observed after 8 years of age, and no 120°＜ATVA＜140°was identified after 12 years [13]. This pattern of higher prevalence of ATVA ≥140° and 120°＜ATVA＜140° in our study extended into adulthood: our previous study in healthy Chinese adults reported a prevalence of 7.5% for ATVA ≥140° and 8.0% for 120°＜ATVA＜140° [24], both exceeding the rates reported by Bächinger et al. (0%) and Jung et al. (4.4%) [8, 25]. (2) Our cohort exhibited greater interindividual variability in ATVA than their previous counterparts, resulting in a wider 90% prediction interval in our study, such that the 90th percentile of ATVA had not fallen below 120° by 19 years of age. (3) Our cohort also demonstrated greater interaural asymmetry: Juliano et al. reported that both ears of each subject fell into the same developmental category, whereas 29.5% of subjects in our study exhibited discordant ATVA categorization between the two ears [13]. The exact mechanisms underlying these disparities remain unclear. The contribution of ethnic background to these disparities cannot be overlooked. In a comparative study of Eskimo, Indian, and White crania using radiographic and direct measurements, Schulter found that 24 of 25 temporal bone morphological parameters exhibited significant differences among the three populations, underscoring the profound impact of race on temporal bone anatomy [16]. Environmental and nutritional factors may also contribute to the observed differences, underscoring the distinctiveness of VA development in this cohort [26, 27].

In addition, we constructed an age-specific ATVA maturation model derived from our subjects, with the 90th percentile serving as the screening threshold. values above this threshold warrant vigilance for potential permanent hypoplasia.

4.2 Association between ATVA and PPD

In the present study, a significant correlation was observed between ATVA and PPD, and PPD demonstrated predictive value for ATVA, serving as a potential adjunctive measure to rule out ATVA ≥ 140°. These findings are broadly consistent with earlier findings, although quantitative discrepancies persist [10, 13, 28]. Specifically, we found that a PPD cutoff of 0.88 mm correctly identified 93.4% of ears with ATVA < 140°, indicating that this threshold effectively excludes ATVA⩾140° while carrying a false-negative rate of 6.6%. Bächinger et al. reported that an PPD > 2 mm excludes MD-hp [10]，while Juliano et al. identified 1.2 mm as the optimal PPD cutoff for distinguishing between the MD-dg and MD-hp endotypes in a study of patients with MD, with a specificity of 0.81, a sensitivity of 0.92, and an AUC of 0.912 [28]. Furthermore, in their investigation of postnatal ATVA development, they found that none of the ears with a PPD ≥ 1.2 mm exhibited a fetal-type ATVA (≥140°) [13] . The aforementioned discrepancies in PPD cutoff values may also be attributable to ethnic differences.

The potential of PPD to serve as a surrogate marker for ATVA ≥ 140° may lie in the shared biological information they provide regarding ES development [8, 15]. PPD indirectly reflects the size of the endolymphatic sac, whereas ATVA ≥ 140° indicates premature developmental arrest of the ES, a condition typically associated with a reduced ES volume and consequently a shorter PPD [11]. Furthermore, given their anatomical proximity within the retro-labyrinthine region, the VA and the adjacent bony structures are likely to develop in a coordinated manner [10, 29]. In summary, PPD is significantly associated with ATVA, rendering it a potential and simpler surrogate marker for endo-typing patients with MD. This is particularly valuable when ATVA measurement is challenging, such as on MRI scans where the VA is sub-optimally visualized, or when the VA is extremely thin and filamentous, as may occur in certain pathological conditions, leading to difficult identification on both CT and MRI [30, 31]. Future studies with larger sample sizes, including both healthy individuals and MD patients, and long-term longitudinal follow-up are warranted to validate these hypotheses, and the relationship between ATVA and PPD requires further investigation**.**

4.3 Association of Peri-VA Pneumatization with ATVA and PPD

Our data demonstrated that the peri-VA air cell system underwent progressive postnatal maturation, with a gradual transition from Type 3 to Type 2 and then to Type 1 with increasing age. Type 3 pneumatization exhibited a significantly higher proportion of ATVA ≥ 140° than Type 1 and Type 2. In addition, a higher degree of pneumatization was associated with a greater PPD, and pneumatization grade partially mediated the age-related increase in PPD. These findings suggest that the degree of pneumatization may serve as a modulating factor in VA and PPD development, and that the three parameters may reflect a coordinated maturation process. These findings are consistent with previous studies [32]. Fujita and Sando demonstrated that

periaqueductal air cells develop postnatally in synchrony with the elongation of the internal auditory canal and the increase in VA volume [12]. Similarly, Nemzek et al., in a histopathological study, observed parallel growth among the VA, the internal auditory canal, and periaqueductal pneumatization [23]. The degree of pneumatization may influence ATVA and PPD development through its effects on dynamic bone remodeling and structural adaptability of the temporal bone [32]. Given that the subarcuate channel, which conveys blood supply to the otic capsule and adjacent structures, varies in length and width depending on the degree of perilabyrinthine pneumatization, it is plausible that peri-VA pneumatization may Dmodulate the vascular microenvironment of the retrolabyrinthine region, thereby influencing the development of both ATVA and PPD [33, 34]. In addition, the formation and expansion of air cells may exert a unique “pushing” or “remodeling” effect on the VA, thereby promoting its maturation, analogous to the way in which enlarging air cells displace the facial nerve posteriorly [35].

Notably, pneumatization and ATVA maturation are not fully synchronized: In this study, ATVA stabilized at 5.93 years, whereas Lee et al. found mastoid pneumatization continues to grow into the third decade in an East Asian population [36, 37]. To the best of our knowledge, this is the first study to report the impact of peri-VA pneumatization on ATVA development. Future studies incorporating quantitative assessment of temporal bone pneumatization, such as three-dimensional reconstruction and volumetric analysis，are warranted to further elucidate the influence of pneumatization on VA development [38].

Our study revealed a significant association between peri-VA pneumatization and ATVA development: 72.7% of ATVA $\geqslant$140 ears showed Type 3 pneumatization, with Type 3 carrying a significantly higher ATVA$\geqslant$140 proportion than Type 1 or Type 2. This suggests that poor pneumatization may restrict normal VA angulation, leading to a ATVA$\geqslant$140. Previous studies have shown that delayed VA development may serve as a mediator of MD pathogenesis and as one of its subtypes [8]. Meanwhile, childhood otitis media with effusion (OME) is known to impair pneumatization. Together, these observations raise the hypothesis that OME may contribute to VA developmental abnormalities, thereby potentially increasing the susceptibility to MD in adulthood [32, 39-41] . future large-scale longitudinal studies are needed to determine whether childhood otitis media with effusion constitutes a risk factor for ATVA maldevelopment and subsequent adult-onset MD.

5. Strength and limitation

To the best of our knowledge, this is the first study to characterize ATVA, peri-VA pneumatization, and PPD development in a healthy Chinese population from birth to adulthood. We identified unique ATVA developmental features in the Chinese population, which may contribute to the establishment of future reference standards for this population, and facilitate

a better understanding of VA maturation and early detection of persistent underdevelopment.

Indeed, this study also has some limitations. This imaging study was conducted in a population from central China and revealed differences compared with previous studies in non-Chinese populations. Further validation in larger normative cohorts from other regions of China is warranted to determine whether anatomical variations contribute differently to the pathogenesis of MD across ethnic groups**.**

6. Conclusion

The maturation of the ATVA is partially coordinated with the development of its surrounding structures. PPD was significantly negatively correlated with ATVA, and a PPD > 0.88 mm showed predictive value for ATVA≥140°. Peri-VA pneumatization continued to mature postnatally and exhibited significant associations with both ATVA and PPD. The interrelationships among these three parameters warrant further investigation.

List of abbreviations

ATVA: angular trajectory of the vestibular aqueduct
CT: computed tomography
ED: endolymphatic duct
ELH: endolymphatic hydrops
ES: endolymphatic sac
GAMLSS: generalized additive models for location, scale and shape
ICC: intraclass correlation coefficient
MD: Meniere's disease
MD-dg: Meniere's disease with degenerative endolymphatic sac pathology
MD-hp: Meniere's disease with hypoplastic endolymphatic sac pathology
NPV: negative predictive value
PPD: vertical part of the posterior semicircular canal—posterior fossa distance
PPV: positive predictive value
REML: restricted maximum likelihood
ROC: receiver operating characteristic
VA: vestibular aqueduct

Declarations

Ethics approval and consent to participate: This retrospective study was reviewed and

approved by the Ethics Committee of Union Hospital, Tongji Medical College, Huazhong University of Science and Technology (Institutional Review Board approval[2023] No. 0354). The study was performed in accordance with the ethical standards of the institutional research committee and with the 1964 Helsinki Declaration and its later amendments. Written informed consent was waived by the Ethics Committee due to the retrospective design of the study and the anonymized nature of the data used.

Consent for publication: Not applicable

Availability of data and materials: The datasets generated and analyzed during the current study are not publicly available due to institutional data protection policies, but can be obtained from the corresponding author upon reasonable request.

Competing interests: The authors declare that they have no competing interests.

Funding: This research was funded by the National Key Research and Development Program of China (2023YFC2508000, and 2023YFC2508001,2023YFC2508400), the Natural Science Foundation of Hubei Province, China of Hubei Province (2021CFB547 and 2025AFB661), and the Science Foun dation of Union Hospital, Tongji Medical College, Huazhong University of Science and Technology (2024XHYN030).

Authors' contributions:

ZX, XS: data analysis and manuscript writing. PL: project development and data collection. XS: data collection and data analysis. QL: methodology and software. HP，KX: software and project administration. YL， YL: investigation and manuscript editing. BL， HP: project development, funding acquisition and manuscript editing. All authors have read and agreed to the published version of the manuscript.

Acknowledgements: We thank all the authors that contributed to this work.

References

1. Merchant SN, Adams JC, Nadol JB, Jr. Pathophysiology of Meniere's syndrome: are symptoms caused by endolymphatic hydrops? Otology & neurotology : official publication of the American Otological Society, American Neurotology Society [and] European Academy of Otology and Neurotology. 2005; doi:10.1097/00129492-200501000-00013
2. Ciuman RR. Communication routes between intracranial spaces and inner ear: function, pathophysiologic importance and relations with inner ear diseases. American journal of otolaryngology. 2009; doi:10.1016/j.amjoto.2008.04.005

3. Lei P, Leng Y, Li J, Zhou R, Liu B. Anatomical variation of inner ear may be a predisposing factor for unilateral Ménière's disease rather than for ipsilateral delayed endolymphatic hydrops. European radiology. 2022; doi:10.1007/s00330-021-08430-7
4. Bächinger D, Egli H, Goosmann MM, Monge Naldi A, Eckhard AH. Immunolocalization of calcium sensing and transport proteins in the murine endolymphatic sac indicates calciostatic functions within the inner ear. Cell and tissue research. 2019; doi:10.1007/s00441-019-03062-2
5. Eckhard AH, Zhu M, O'Malley JT, Williams GH, Loffing J, Rauch SD, Nadol JB, Jr., Liberman MC, Adams JC. Inner ear pathologies impair sodium-regulated ion transport in Meniere's disease. Acta neuropathologica. 2019; doi:10.1007/s00401-018-1927-7
6. Bloch SL, Friis M. Objective measurement of the human endolymphatic sac dimensions in Ménière's disease. Otology & neurotology : official publication of the American Otological Society, American Neurotology Society [and] European Academy of Otology and Neurotology. 2011; doi:10.1097/MAO.0b013e31822e967f
7. Friberg U, Rask-Andersen H. Vascular occlusion in the endolymphatic sac in Meniere's disease. The Annals of otology, rhinology, and laryngology. 2002; doi:10.1177/000348940211100308
8. Bächinger D, Luu NN, Kempfle JS, Barber S, Zürrer D, Lee DJ, Curtin HD, Rauch SD, Nadol JB, Jr., Adams JC *et al.* Vestibular Aqueduct Morphology Correlates With Endolymphatic Sac Pathologies in Menière's Disease-A Correlative Histology and Computed Tomography Study. Otology & neurotology : official publication of the American Otological Society, American Neurotology Society [and] European Academy of Otology and Neurotology. 2019; doi:10.1097/mao.0000000000002198
9. Bächinger D, Brühlmann C, Honegger T, Michalopoulou E, Monge Naldi A, Wettstein VG, Muff S, Schuknecht B, Eckhard AH. Endotype-Phenotype Patterns in Meniere's Disease Based on Gadolinium-Enhanced MRI of the Vestibular Aqueduct. Frontiers in neurology. 2019; doi:10.3389/fneur.2019.00303
10. Bächinger D, Filidoro N, Naville M, Juchler N, Kurtcuoglu V, Nadol JB, Jr., Schuknecht B, Kleinjung T, Veraguth D, Eckhard AH. Radiological feature heterogeneity supports etiological diversity among patient groups in Meniere's disease. Scientific reports. 2023; doi:10.1038/s41598-023-36479-5
11. Watzke D, Bast TH. The development and structure of the otic [endolymphatic) sac. The Anatomical record. 1950; doi:10.1002/ar.1091060305
12. Fujita S, Sando I. Postnatal development of the vestibular aqueduct in relation to the internal auditory canal. Computer-aided three-dimensional reconstruction and measurement study. The Annals of otology, rhinology, and laryngology. 1994; doi:10.1177/000348949410300910
13. Juliano AF, Naik PK, Romo LV, Huey N, Lin KY, Bächinger D, Robson CD, Eckhard AH. Postnatal Development of the Vestibular Aqueduct Trajectory on CT: Establishing Age-Specific Norms to Distinguish Normal from Arrested

(Hypoplastic) Development. AJNR American journal of neuroradiology. 2026; doi:10.3174/ajnr.A8933
14. Stahle J, Wilbrand HF. The temporal bone in patients with Meniere's disease. Acta oto-laryngologica. 1983; doi:10.3109/00016488309130919
15. Mateijsen DJ, Van Hengel PW, Krikke AP, Van Huffelen WM, Wit HP, Albers FW. Three-dimensional Fourier transformation constructive interference in steady state magnetic resonance imaging of the inner ear in patients with unilateral and bilateral Menière's disease. Otology & neurotology : official publication of the American Otological Society, American Neurotology Society [and] European Academy of Otology and Neurotology. 2002; doi:10.1097/00129492-200203000-00017
16. Schulter FP. A comparative study of the temporal bone in three populations of man. American journal of physical anthropology. 1976; doi:10.1002/ajpa.1330440309
17. Nordström CK, Laurell G, Rask-Andersen H. The Human Vestibular Aqueduct: Anatomical Characteristics and Enlargement Criteria. Otology & neurotology : official publication of the American Otological Society, American Neurotology Society [and] European Academy of Otology and Neurotology. 2016; doi:10.1097/mao.0000000000001203
18. Watanabe S, Schneider T, Amagasaki K, Nakaguchi H, Unterberg A, Dao Trong P. Differences in mastoid pneumatization between Asians and Caucasians. Journal of clinical neuroscience : official journal of the Neurosurgical Society of Australasia. 2023; doi:10.1016/j.jocn.2023.01.009
19. Albers FW, Van Weissenbruch R, Casselman JW. 3DFT-magnetic resonance imaging of the inner ear in Meniére's disease. Acta oto-laryngologica. 1994; doi:10.3109/00016489409126111
20. Marmolejo-Ramos F, Tejo M, Brabec M, Kuzilek J, Joksimovic S, Kovanovic V, González J, Kneib T, Bühlmann P, Kook L *et al*. Distributional regression modeling via generalized additive models for location, scale, and shape: An overview through a data set from learning analytics. Wiley interdisciplinary reviews Data mining and knowledge discovery. 2023; doi:10.1002/widm.1479
21. Rijnhart JJM, Twisk JWR, Valente MJ, Heymans MW. Time lags and time interactions in mixed effects models impacted longitudinal mediation effect estimates. Journal of clinical epidemiology. 2022; doi:10.1016/j.jclinepi.2022.07.004
22. Maślanka M, Skadorwa T, Ciszek B. Postnatal development of the subarcuate fossa and subarcuate canaliculus-a computed tomographic study. Surgical and radiologic anatomy : SRA. 2018; doi:10.1007/s00276-018-2045-x
23. Nemzek WR, Brodie HA, Chong BW, Babcook CJ, Hecht ST, Salamat S, Ellis WG, Seibert JA. Imaging findings of the developing temporal bone in fetal specimens. AJNR American journal of neuroradiology. 1996;
24. Xia K, Lei P, Liu Y, Chen C, Xiao H, Leng Y, Liu B. Angular Trajectory of the Vestibular Aqueduct in a Cohort of Chinese Patients with Unilateral Ménière's Disease: Association with Other Imaging Indices and Clinical Profiles.

Biomedicines. 2024; doi:10.3390/biomedicines12092008
25. Jung D, Nagururu N, Hui F, Pearl MS, Carey JP, Ward BK. 2D Measurements of the Angle of the Vestibular Aqueduct Using CT Imaging. Brain sciences. 2022; doi:10.3390/brainsci13010047
26. Aladeyelu OS, Olaniyi KS, Olojede SO, Mbatha WE, Sibiya AL, Rennie CO. Temporal bone pneumatization: A scoping review on the growth and size of mastoid air cell system with age. PloS one. 2022; doi:10.1371/journal.pone.0269360
27. Lee DH, Kim MJ, Lee S, Choi H. Anatomical Factors Influencing Pneumatization of the Petrous Apex. Clinical and experimental otorhinolaryngology. 2015; doi:10.3342/ceo.2015.8.4.339
28. Juliano AF, Lin KY, Shekhrajka N, Shin D, Rauch SD, Eckhard AH. Retrolabyrinthine Bone Thickness as a Radiologic Marker for the Hypoplastic Endotype in Menière Disease. AJNR American journal of neuroradiology. 2024; doi:10.3174/ajnr.A8339
29. Liang C, Profico A, Buzi C, Khonsari RH, Johnson D, O'Higgins P, Moazen M. Normal human craniofacial growth and development from 0 to 4 years. Scientific reports. 2023; doi:10.1038/s41598-023-36646-8
30. Jutel M, Agache I, Zemelka-Wiacek M, Akdis M, Chivato T, Del Giacco S, Gajdanowicz P, Gracia IE, Klimek L, Lauerma A *et al*. Nomenclature of allergic diseases and hypersensitivity reactions: Adapted to modern needs: An EAACI position paper. Allergy. 2023; doi:10.1111/all.15889
31. Dauphin D, Laffont J, Garand G, Reynaud J. Menière's disease, petrous bone tomography. A new radiographic sign? Neuroradiology. 1981; doi:10.1007/bf00344604
32. Zhao P, Ding H, Lv H, Li J, Liu X, Yang Z, Wang Z. Growth pattern of temporal bone pneumatization: a computed tomography study with consecutive age groups. Surgical and radiologic anatomy : SRA. 2019; doi:10.1007/s00276-018-2113-2
33. Wilbrand H, Rauschning W, Ruhn G. The subarcuate fossa and channel. A radioanatomic investigation. Acta radiologica: diagnosis. 1986; doi:10.1177/028418518602700604
34. Russo C, Coluccino S, Sarno M, Pascarella A, Casale A, De Lucia A, Spennato P, Cascone D, Cicala D, Russo C *et al*. Acute Otomastoiditis in Children: An Observational Study on the Role of Mastoid Morphology in the Development of Intracranial Complications. Journal of clinical medicine. 2025; doi:10.3390/jcm14217715
35. Dai P, Zhang T, Wang K, Song J, Qian W, Wang Z. Positional relationship between the facial nerve and other structures of the temporal bone. The Journal of laryngology and otology. 2004; doi:10.1258/002221504772784540
36. Lee DH, Jun BC, Kim DG, Jung MK, Yeo SW. Volume variation of mastoid pneumatization in different age groups: a study by three-dimensional reconstruction based on computed tomography images. Surgical and radiologic anatomy : SRA. 2005; doi:10.1007/s00276-004-0274-7

37. Campostrini C, Wojciechowski T, Szopiński K, Fermi M. Radioanatomical assessment of the subtympanic sinus and its relationship to facial nerve position and temporal bone pneumatization in adults: CT study. Surgical and radiologic anatomy : SRA. 2026; doi:10.1007/s00276-026-03907-w
38. Byun SW, Lee SS, Park JY, Yoo JH. Normal Mastoid Air Cell System Geometry: Has Surface Area Been Overestimated? Clinical and experimental otorhinolaryngology. 2016; doi:10.21053/ceo.2016.9.1.27
39. Shatz A, Sadé J. Correlation between mastoid pneumatization and position of the lateral sinus. The Annals of otology, rhinology, and laryngology. 1990; doi:10.1177/000348949009900213
40. Han SJ, Song MH, Kim J, Lee WS, Lee HK. Classification of temporal bone pneumatization based on sigmoid sinus using computed tomography. Clinical radiology. 2007; doi:10.1016/j.crad.2007.04.019
41. Turgut S, Tos M. Correlation between temporal bone pneumatization, location of lateral sinus and length of the mastoid process. The Journal of laryngology and otology. 1992; doi:10.1017/s0022215100119942

Supplementary Files

This is a list of supplementary files associated with this preprint. Click to download.

- Supplementarymaterial.docx